



## Rigorous simulation of nonlinear optomechanical coupling in micro- and nano-structured resonant cavities

Matteo Stocchi, Davide Mencarelli, Yan Pennec, Bahram Djafari-Rouhani & Luca Pierantoni

To cite this article: Matteo Stocchi, Davide Mencarelli, Yan Pennec, Bahram Djafari-Rouhani & Luca Pierantoni (2018) Rigorous simulation of nonlinear optomechanical coupling in micro- and nano-structured resonant cavities, International Journal of Optomechatronics, 12:1, 11-19, DOI: [10.1080/15599612.2018.1459977](https://doi.org/10.1080/15599612.2018.1459977)

To link to this article: <https://doi.org/10.1080/15599612.2018.1459977>



Published with license by Taylor & Francis©  
2018 Matteo Stocchia, Davide Mencarelli,  
Yan Pennec, Bahram Djafari-Rouhani and  
Luca Pierantoni



Published online: 04 Jun 2018.



Submit your article to this journal [↗](#)



Article views: 2




View related articles [↗](#)



View Crossmark data [↗](#)

# Rigorous simulation of nonlinear optomechanical coupling in micro- and nano-structured resonant cavities

Matteo Stocchi<sup>a</sup> , Davide Mencarelli<sup>a,b</sup>, Yan Pennec<sup>c</sup>, Bahram Djafari-Rouhani<sup>c</sup> and Luca Pierantoni<sup>a,b</sup>

<sup>a</sup>Department of Information Engineering, Marche Polytechnic University, Ancona, Italy; <sup>b</sup>Laboratori Nazionali di Frascati (LNF), Istituto Nazionale di Fisica Nucleare (INFN), Frascati, Roma, Italy; <sup>c</sup>Institut d'Electronique, de Micro électronique et de Nanotechnologie, UMR CNRS 8520, Université de Lille, France

## ABSTRACT

A numerical method aimed to predict the optomechanical dynamics in micro- and nano-structured resonant cavities is introduced here. The rigorousness of it is ensured by exploiting the harmonic version of the transformation optics (TO) technique and by considering all the energy-transduction contributions of electrostriction, radiation pressure, photoelasticity and moving boundaries. Since our full-wave approach implements a multi-modal analysis and also considers material losses, from both a mechanical and an optical point of view, a considerable step further has been made in respect to the standard optomechanical perturbative theory. The efficiency and the versatility of the strategy are tested by analysing the optomechanical behaviour of a corrugated Si-based nanobeam and comparing numerical results to experimental ones from the literature.

## KEYWORDS

Optomechanics; stimulated Brillouin scattering; numerical analysis; full-wave simulation; moving boundary effect

## 1. Introduction

In the recent past, the interlacing between optical cavities and mechanical systems has given rise to a rapid development of the research branch called cavity optomechanics which aims, by the means of a high-Q resonant recirculation, to confine light into small volumes.<sup>[1–4]</sup> The intent of an optomechanical system is to investigate the interaction of light with a mechanical oscillator, and its highly interdisciplinary nature leads to several potential applications in various fields of research, especially in quantum processing.<sup>[5–9]</sup> It has been shown that the combination of both optical and mechanical interactions guarantees the most successful exploitation of mechanical vibrations for the managing of quantum phenomena through phonon-assisted optical or sideband transitions, as demonstrated in trapped ions<sup>[10,11]</sup> and, more recently, in cavity optomechanics.<sup>[12–19]</sup> Focusing on the latter, optomechanical micro-cavities can also serve as a possible concept to provide new functionalities, applications and opportunities beyond standard technology, owing to phonon propagation, generation and processing.<sup>[20,21]</sup> In this contribution, we present a fully coupled numerical approach which, combining the two exerted physics of mechanics and optics, accurately predicts the optomechanical dynamics in micro-structured resonant cavities.<sup>[22]</sup> The rigorousness of such analysis is ensured by considering all the four main energy-transduction contributions.<sup>[23]</sup> Referring to the two inserts of Figure 1, the radiation pressure and

**CONTACT** Matteo Stocchi  [m.stocchi@pm.univpm.it](mailto:m.stocchi@pm.univpm.it)  Department of Information Engineering, Marche Polytechnic University, Ancona, Italy

Color versions of one or more of the figures in this article can be found online at [www.tandfonline.com/uopt](http://www.tandfonline.com/uopt).

Published with license by Taylor & Francis © 2018 Matteo Stocchia, Davide Mencarelli, Yan Pennec, Bahram Djafari-Rouhani and Luca Pierantoni. This is an Open Access article distributed under the terms of the Creative Commons Attribution-NonCommercial-NoDerivatives License (<http://creativecommons.org/licenses/by-nc-nd/4.0/>), which permits non-commercial re-use, distribution, and reproduction in any medium, provided the original work is properly cited, and is not altered, transformed, or built upon in any way.

### Nomenclature

TO	Transformation optics	$\mathbf{F}_{ES,V}$	Electrostrictive force, boundary, $\text{N}/\text{m}^2$
$\omega_1$	Angular frequency, optical pump, Hz	$f_m$	Mechanical frequency, Hz
$\omega_2$	Angular frequency, scattered field, Hz	$u_0$	Initial displacement, m
$\Omega$	Mechanical angular frequency, Hz	$m_{\text{eff}}$	Effective mass
$\mathbf{u}$	Mechanical displacement, m	$\bar{\bar{g}}$	Metric tensor
$\rho_0$	Mass density, $\text{Kg}/\text{m}^3$	$\bar{\bar{F}}$	Deformation gradient
$\mathbf{F}_{RP}$	Radiation pressure force, $\text{N}/\text{m}^2$		
$\mathbf{F}_{ES,V}$	Electrostrictive force, volume, $\text{N}/\text{m}^3$		

the electrostriction constitutes the forces wielded by the E-field on the matter, whereas the photoelasticity describes the perturbation of the electromagnetic radiation caused by the presence of the mechanical wave. Special considerations are then required for what concerns the so called *moving boundary* effect, i.e. the boundary deformation caused by the space-time varying pressure field that perturbs the electromagnetic boundary conditions. Specifically, the Eulerian coordinates in which the Maxwell equations are solved are not able to take into account for the mechanical displacement, defined, in turn, in Lagrangian coordinates. As a matter of fact, the just reported limitation can be numerically significant in case of nano-scale cavities. The transformation optics (TO)<sup>[24,25]</sup> method represents an elegant and efficient solution to the addressed problem. According to its original concept, TO is an analytical tool that facilitates the design of a variety of optical devices (lenses, phase shifters, deflectors, etc.) by deforming the coordinate system, warping space to control the trajectories of the electromagnetic radiation. Such alteration then turns into a change of the electromagnetic material parameters such as the permittivity  $\epsilon$  and the permeability  $\mu$ . For the special case of optomechanics, TO is used to take into account for the time-varying boundaries of the domain under investigation,<sup>[26]</sup> making then possible to consider the moving boundary effect by means of a modified version of the standard Helmholtz equation.

## 2. Theoretical background

From an analytical point of view, optomechanics is described by the combination between the continuum mechanical physics and the classic electrodynamics. The foundations of the considered phenomena rely on the relation as follows:<sup>[27]</sup>

$$\omega_1 = \omega_2 \pm \Omega, \quad (1)$$

where  $\Omega$  is the mechanical frequency and  $\omega_{1,2}$  are the optical ones, respectively, of the pumped and of the scattered light. Such relation states the exchange of energy between the provided electromagnetic radiation and the mechanical motion, also defining the matching condition for the time-dependent source terms that, as we shall see shortly, enter in the ruling equations of the physics of interest. A general mechanical wave, whether is it confined in a mechanical cavity or free to propagate, is efficiently described in terms of the displacement  $\mathbf{u}$ , which satisfies the conservation law of the linear momentum<sup>[28]</sup>

$$\rho_0 \Omega^2 \mathbf{u} + \nabla_{\mathbf{X}} \cdot (\bar{\bar{F}}\bar{\bar{S}}) = -\mathbf{F}_{RP} - \mathbf{F}_{ES,V} - \mathbf{F}_{ES,B}, \quad (2)$$

where  $\rho_0$  the mass density of the undeformed configuration,  $\bar{\bar{F}}$  the deformation gradient tensor,  $\bar{\bar{S}}$  the second Piola-Kirchhoff tensor and  $\nabla_{\mathbf{X}}$  indicates the nabla operator expressed in Lagrangian coordinates. The right-side of Equation (2) introduces two of the four aforementioned coupling parameters of an optomechanical phenomenon, i.e. the radiation pressure  $\mathbf{F}_{RP}$  and the electrostrictive forces  $\mathbf{F}_{ES,V}$ ,  $\mathbf{F}_{ES,B}$ , splitted for numerical purpose in their volumetric and perimetric

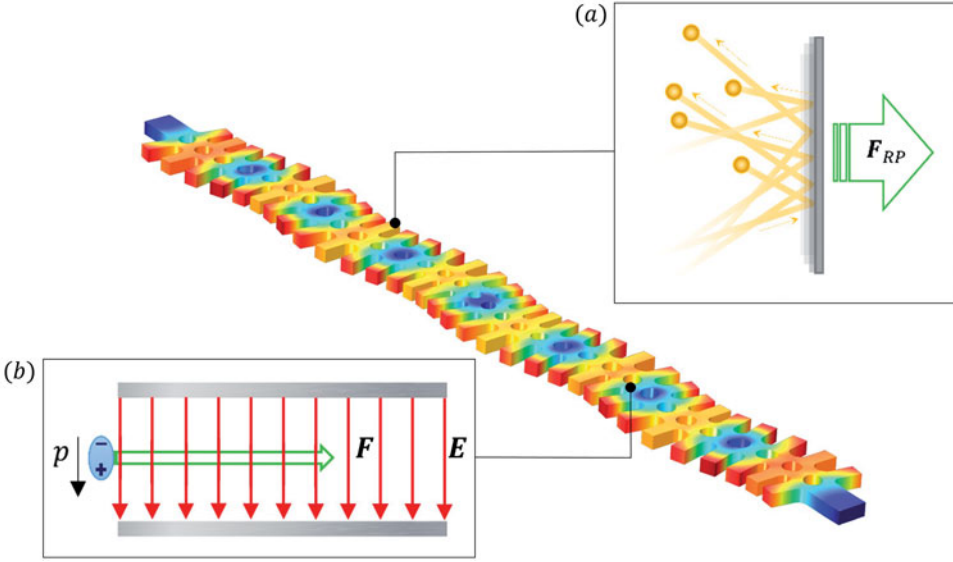


**Figure 1.** Visualisation of an optomechanical interaction: the incident electromagnetic radiation generates the two force-like optic contributions of (a) radiation pressure and (b) electrostriction, here presented as the force exerted by the E-field on a molecule.

contributions.<sup>[29]</sup> Two additional mechanical quantities must be taken into account: the effective mass  $m_{eff}$ <sup>[30]</sup> so that it is possible to study the non-ideal oscillating system as a simple harmonic oscillator, and the thermally induced initial displacement  $u_0$ , essential for having an initial condition for the mechanical module. The latter is given by the following:<sup>[31]</sup>

$$u_0^2 \sim \frac{4k_B T}{m_{eff} f_m^2} \quad (3)$$

and implemented in the fem-solver as a pre-existing condition for the mechanical motion. As afore-stated, in a standard full-wave simulator Maxwell equations are solved in Eulerian coordinates, that are not able to automatically account for the effect of the displacement on the boundaries. TO offers a valid solution to overcome such a problem. According to what has been developed by Zecca et al.,<sup>[26]</sup> the modified version of the Helmholtz equations accounting for both the photoelastic and the moving boundary effects are given as the following:

$$\nabla \times \bar{\bar{A}}^{-1} \nabla \times \mathbf{E}_1 - \omega_1^2 \bar{\bar{C}} \mathbf{E}_1 = \omega_1^2 [\bar{\bar{K}} \mathbf{E}_1 + (\bar{\bar{D}} + \bar{\bar{L}}) \mathbf{E}_2] - i\omega_1 \nabla \times (\bar{\bar{A}}^{-1} \bar{\bar{B}} \mathbf{H}_2). \quad (4)$$

$$\nabla \times \bar{\bar{A}}^{-1} \nabla \times \mathbf{E}_2 - \omega_2^2 \bar{\bar{C}} \mathbf{E}_2 = \omega_2^2 [\bar{\bar{K}} \mathbf{E}_2 + (\bar{\bar{D}}^* + \bar{\bar{L}}^2) \mathbf{E}_1] - i\omega_2 \nabla \times (\bar{\bar{A}}^{-1} \bar{\bar{B}}^* \mathbf{H}_1). \quad (5)$$

To derive a more compact form of the equations, the following second rank tensors have been introduced<sup>[26]</sup>

$$\bar{\bar{A}} = \bar{\bar{g}}_0 \mu, \quad \bar{\bar{B}} = \bar{\bar{g}}_1 \mu, \quad \bar{\bar{C}} = \bar{\bar{g}}_0 \epsilon, \quad \bar{\bar{D}} = \bar{\bar{g}}_1 \epsilon, \quad \bar{\bar{K}} = \frac{\epsilon_0}{2} (\bar{\bar{g}}_1 \bar{\bar{\Delta}} \epsilon^* + \bar{\bar{g}}_1^* \bar{\bar{\Delta}} \epsilon), \quad \bar{\bar{L}} = \frac{\epsilon_0}{2} (\bar{\bar{g}}_2 \bar{\bar{\Delta}} \epsilon^* + \bar{\bar{g}}_2^* \bar{\bar{\Delta}} \epsilon).$$

where  $\mathbf{E}_{1,2}$  are the pumped/scattered electric fields,  $\bar{\bar{\Delta}} \epsilon$  the photoelastic contribution and  $\bar{\bar{g}}$  has been defined as the metric tensor, composed of seven terms of different harmonics directly derived from the TO procedure.

$$\bar{\bar{g}} = \frac{\bar{\bar{F}} \bar{\bar{F}}}{\det \bar{\bar{F}}} = \sum_{n=-3}^3 \bar{\bar{g}}_n e^{in\Omega t}. \quad (6)$$

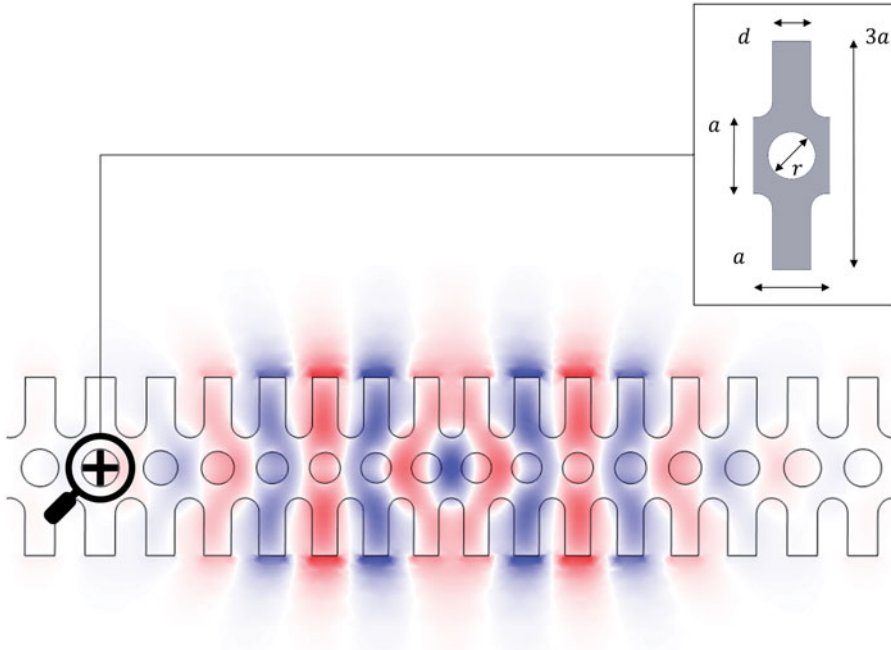


**Figure 2.** Spatial E-field distribution of the considered optical mode with a focus (see the insert) on the unit cell of the optomechanical crystal. The nominal geometrical values of the latter are  $a=500$  nm,  $r=150$  nm and  $d=250$  nm, with a thickness of 220 nm.

### 3. Validation of the method

In what follows, a validation of the proposed predictive model, pursued by regaining and expanding the experimental results obtained in the work by Navarro-Urrios et al.<sup>[32]</sup> concerning the observation of a breathing mechanical mode at 5.5 GHz in a 1D corrugated *Si*-based nanobeam, will be given. Such mechanical mode optomechanically interacts with the optical resonance, of which the E-field norm is shown in Figure 2, through a strong dynamical back-action effect at a room temperature. The unit cell of the optomechanical crystal is a *Si* parallelogram which presents a cylindrical hole in the centre and two symmetric stubs on the side. Such a structure exhibits a full phononic band gap around 4 GHz, as verified in the work by Gomis-Bresco et al.<sup>[33]</sup> The geometry of the optomechanical cavity is composed of two mirror regions on the right and on the left sides of the structure which enclose a section where the pitches, the radius and the stubs length of the unit cells have been scaled in a quadratic way towards the centre, with a maximum geometrical reduction with respect to the mirror cells of 17%. Both doping and resistivity  $\rho$  of the crystalline silicon layer of which the cavity is made (respectively of  $\sim 1-10$   $\Omega\text{cm}^{-1}$  and  $\sim 10^{15}$   $\text{cm}^{-3}$ ) have been incorporated into the conductivity  $\sigma$ , while the anisotropy is modelled by mean of a non-diagonal elasticity matrix. In addition, an isotropic loss factor of 0.001 has been considered. A first remarkable difference between the experimental observations and our predictive model is the frequency in which the chosen optical resonance falls: according to the measurements taken by Navarro-Urrios et al.,<sup>[32]</sup> the latter happens to be at  $f_{opt,measured} \sim 190$  THz, whereas, according to our calculations,  $f_{opt,calculated} = 149.17$  THz. Such a difference relies on the 2D-environment in which our simulations are carried out, since the loss of the electromagnetic fields confinement in the missing third dimension causes a shift in all the optical resonance frequencies. As we shall see in what follows, such frequency-mode shifting also happens when it comes to consider the mechanical resonances, although not as marked as in the optical case. From the experimental point of view, as a result of the excitation of the considered

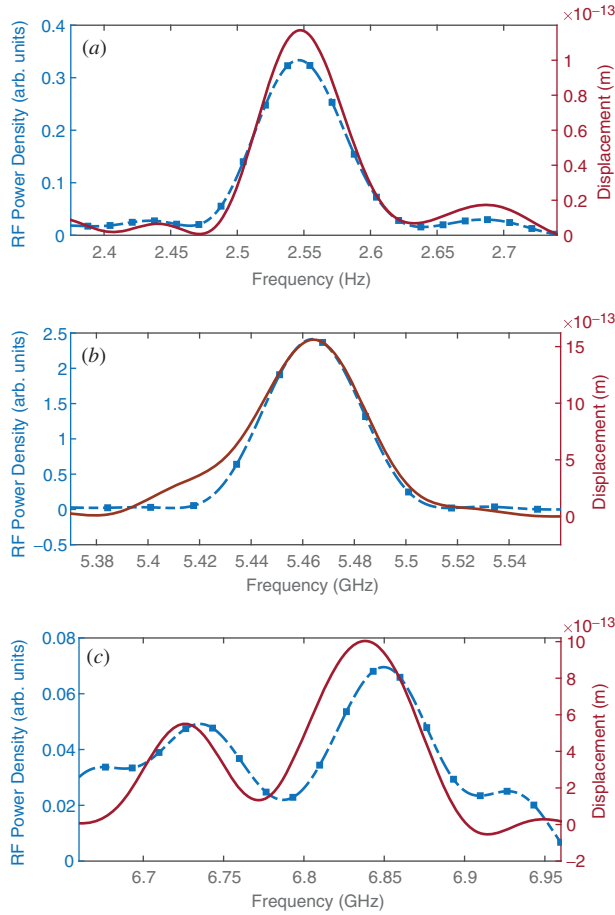


**Figure 3.** Qualitative comparison between theoretical (red dots, m) and experimental (blue triangles, *arb.units*) data, as reported in <sup>[32]</sup>, for three different range of frequencies: (a) 2.35–2.7 GHz, (b) 5.36–5.56 GHz and (c) 6.65–6.95 GHz.

optical mode, a strong RF transduced signal is observed corresponding to mechanical modes distributions over a spectral range between 10 MHz and 9 GHz.<sup>[32]</sup> The numerical analysis gives, in turn, the effective enhancement of the displacement associated to the considered mechanical resonances. Although the extrapolated data are not comparable in absolute terms, the juxtaposition of their trends on three different intervals of the frequency spectrum of the mechanical modes, as reported in Figure 3, clearly shows a good resemblance. In particular, the four measured peaks in the RF power density spectrum<sup>[32]</sup> falling at the frequencies of  $f_{m,1} \sim 2.5$  GHz,  $f_{m,2} \sim 5.5$  GHz,  $f_{m,3} \sim 6.65$  GHz and  $f_{m,4} \sim 6.75$  GHz are acceptably matched by the ones numerically computed. As aforesaid, also in this case a frequency compensation of  $\Delta f = 0.5$  GHz has been considered in order to get rid of the limiting bidimensional environment in which the calculations have been conducted. Focusing on the mechanical mode under investigation, if we consider the thermal displacement  $u_0 = 3.21 \cdot 10^{-13}$  m ( $T = 300$  K) and an exciting optical power of  $P_{opt} = 20$  mW, the optomechanical interaction carried out by means of our numerical simulations leads to a final displacement of  $u = 1.55 \cdot 10^{-12}$  m, as shown in Figure 3(b). For the sake of completeness, the spatial displacement field distribution associated to the four mechanical modes taken into consideration is plotted in Figure 4, which also indicates the related parameters of the quality factor  $Q_m$ , the effective mass  $m_{eff}$  and the optomechanical coupling rate  $g_{OM}$ , derived from the classical perturbative approach.<sup>[34]</sup> Figure 5 shows the modulus of two forces, exerted by the electromagnetic field, of electrostriction (considered both on the boundaries and on the whole

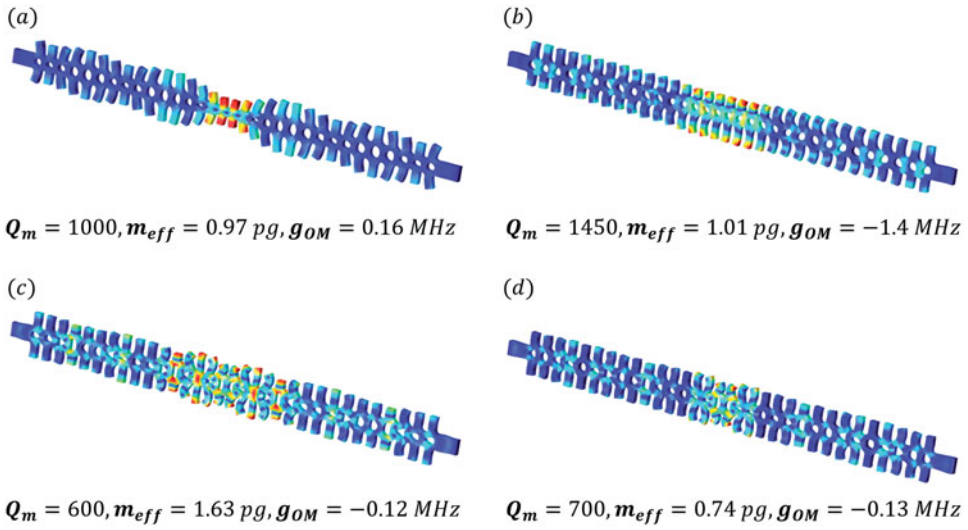


**Figure 4.** Spatial displacement field distribution and parameters of optomechanical interest (effective mass  $m_{eff}$ , quality factor  $Q_m$  and optomechanical coupling rate  $g_{OM}$ ) of the mechanical modes resonating at (a) 2.08 GHz, (b) 5.02 GHz, (c) 6.07 GHz and (d) 6.17 GHz related to the peaks shown in Figure 3(a)–(c).

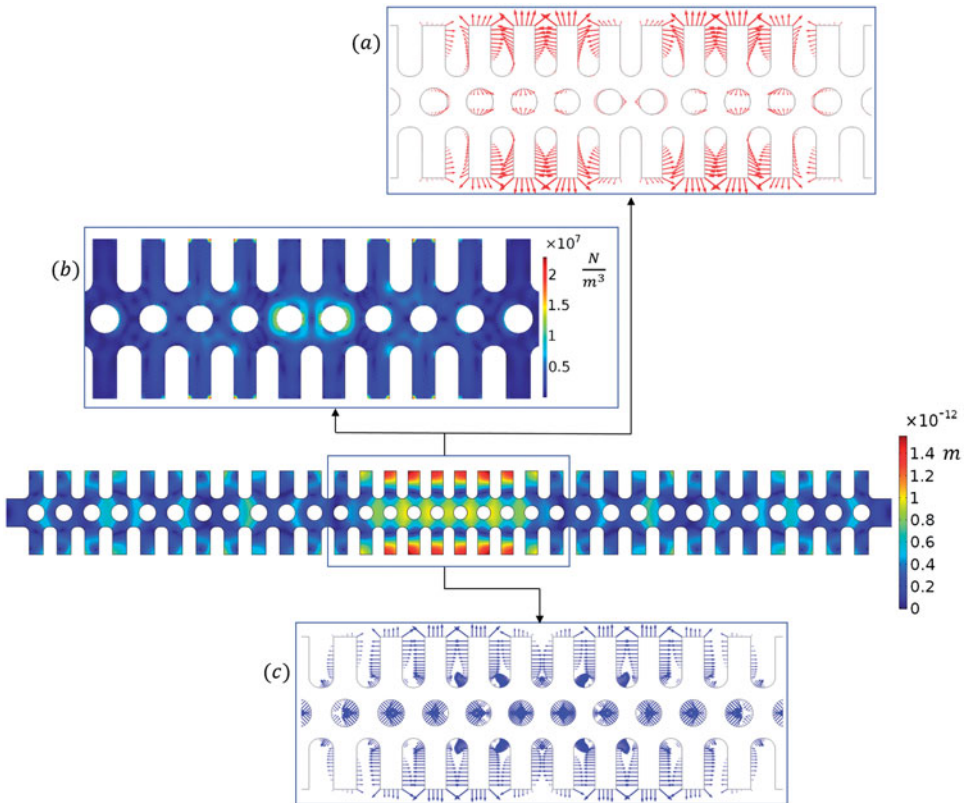


**Figure 5.** Evaluation and visualisation of the optical contributions related to the chosen mechanical resonating mode ( $f_m = 5.02 \text{ GHz}$ ): the electrostrictive force acting on both (a) the boundaries and (b) the volume of the optomechanical cavity and (c) the radiation pressure.

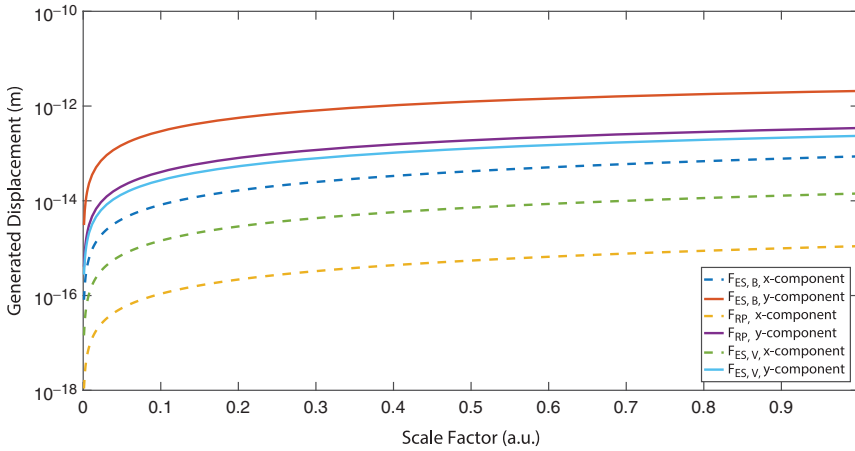


**Figure 6.** Displacement generated from the single components ( $x$  and  $y$ ) of the three force contributions  $F_{ES,B}$ ,  $F_{ES,V}$  and  $F_{RP}$  taken individually.

volume of the cavity) and radiation pressure and also the displacement  $u$ , generated from the optomechanical interaction. It is evident that the highest optically exerted forces occur in correspondence of abrupt discontinuities, which is actually where the displacement field of the mechanical mode under analysis reaches its maximum values. Such congruency constitutes the main reason why the optomechanical coupling between the two resonating modes, i.e. the optical and the mechanical one, is particularly high. Further considerations can be made on the effective contribution exerted by the three aforementioned forces by simply taking them individually, as done in Figure 6. By evaluating the single effects of the various force components  $F_{ES,B}^x$ ,  $F_{ES,B}^y$ ,  $F_{ES,V}^x$ ,  $F_{ES,V}^y$ ,  $F_{RP}^x$  and  $F_{RP}^y$  weighed by a scale factor, i.e. a multiplier coefficient going from 0 to 1, it is in the first instance possible to notice that the transversal polarization of the optical mode makes the  $y$  contributions much more effective than the  $x$  ones. Secondly, given the field configuration of the mechanical resonance under analysis, the boundary forces generate higher values of the displacement  $u$  in respect to the volume ones. According to our calculations, the electrostrictive boundary force results to be considerably higher than the radiation pressure one: the peak values are found to be of, respectively, 7.22 and 2.78 Pa. Additionally, by observing the values of the maximum displacement  $Max(u)$  resulting from the application of the aforelisted individual contributions (especially the one coming from the  $y$  component of the electrostrictive boundary force  $F_{ES,B}^y$ ;  $Max(u) = 2.08 \cdot 10^{-12}$  m) and the one coming from the fully coupled optomechanical approach ( $Max(u) = 1.55 \cdot 10^{-12}$  m), It turns out that there is no visible cumulative effect, but rather that the electrostrictive and the radiation pressure forces seem to compensate for the effects of each other<sup>[35]</sup>.

#### 4. Conclusion


In this contribution, a fully coupled numerical approach which accurately predicts the optomechanical dynamics in micro-structured resonant cavities has been presented. The results coming from the method have been tested with respect to the experimental ones from the literature, and a good agreement between the two has been shown. Our method considerably differs from the standard perturbative analysis<sup>[34]</sup> by giving the effective final displacement of the mechanical resonating mode under investigation caused by the optical excitation and, also, the possibility to evaluate the various optomechanical interaction forces as the electrostriction and the radiation pressure. A further addition concerns the possibility of conducting a multi-modal analysis and taking into account for the material losses, both in mechanical and optical terms, which is of key importance in order to correctly characterise the optomechanical phenomenon.



## Acknowledgements

This research is supported by the European Project All-Phononic circuits Enabled by Opto-mechanics PHENOMEN, H2020 FETOPEN 2014-2015-RIA, n.713450.

## ORCID

Matteo Stocchi  <http://orcid.org/0000-0002-6027-6012>

## References

- [1] AspelmeyerGrblacher, M.; Hammerer, S.K.; Kiesel, N. Quantum optomechanics throwing a glance. *J. Opt. Soc. Am.* **2010**, *B27*, 189–197.
- [2] Aspelmeyer, M.; Kippenberg, T.J.; Marquardt, F. Cavity optomechanics. *Rev. Mod. Phys.* **2014**, *86*, 1391.
- [3] Maldovan, M. Sound and heat revolutions in phononics. *Nature* **2013**, *503*, 209–217.
- [4] Rath, P.; Ummethala, S.; Diewald, S.; Lewes-Malandrakis, G.; Brink, D.; Heidrich, N.; Nebel, C.; Pernice, W.H.P. Diamond electro-optomechanical resonators integrated in nanophotonic circuits. *Appl. Phys. Lett.* **2014**, *105*, 251102.
- [5] Gustafsson, M.V.; Aref, T.; Kockum, A.F.; Ekstrom, M.K.; Johansson, G.; Delsing, P. Propagating phonons coupled to an artificial atom. *Science* **2014**, *346*, 207.
- [6] Schuetz, M.J.A.; Kessler, E.M.; Giedke, G.; Vandersypen, L.M.K.; Lukin, M.D.; Cirac, J.I. Universal quantum transducers based on surface acoustic waves. *Phys. Rev. X* **2015**, *5*, 031031.
- [7] MacQuarrie, E.R.; Gosavi, T.A.; Jungwirth, N.R.; Bhawe, S.A.; Fuchs, G.D. Mechanical spin control of nitrogen-vacancy centers in diamond. *Phys. Rev. Lett.* **2013**, *111*, 227602.
- [8] Soykal, O.O.; Ruskov, R.; Tahan, C. Sound-based analogue of cavity quantum electrodynamics in silicon. *Phys. Rev. Lett.* **2011**, *107*, 235502.
- [9] Bennett, S.D.; Yao, N.Y.; Otterbach, J.; Zoller, P.; Rabl, P.; Lukin, M.D. Phonon-induced spin-spin interactions in diamond nanostructures: Application to spin squeezing. *Phys. Rev. Lett.* **2013**, *110*, 156402.
- [10] Leibfried, D.; Blatt, R.; Monroe, C.; Wineland, D. Quantum dynamics of single trapped ions. *Rev. Mod. Phys.* **2003**, *75*, 281.
- [11] Wineland, D.J. Nobel lecture: Superposition, entanglement, and raising Schrodinger's cat. *Rev. Mod. Phys.* **2013**, *85*, 1103.
- [12] Aspelmeyer, M.; Kippenberg, T.J.; Marquardt, F. Cavity optomechanics. *Rev. Mod. Phys.* **2014**, *86*, 1391.
- [13] Metcalfe, M. Applications of cavity optomechanics. *Appl. Phys. Rev.* **2014**, *1*, 031105.
- [14] Gavartin, E.; Braive, R.; Sagnes, I.; Arcizet, O.; Beveratos, A.; Kippenberg, T.J.; Robert-Philip, I. Optomechanical coupling in a two-dimensional photonic crystal defect cavity. *Phys. Rev. Lett.* **2011**, *106*, 203902.
- [15] Kuhn, A.; Bahriz, G.; Ducloux, M.; Chartier, O.C.; Traon, O.; Briant, L.T.; Cohadon, P.; Heidmann, F.; Michel, A.; Pinard, C.L.; Flaminio, R. A micropillar for cavity optomechanics. *Appl. Phys. Lett.* **2011**, *99*, 121103.
- [16] Kuhn, A.G.; Teissier, J.; Neuhaus, L.; Zerkani, S.; van Brackel, E.; Deléglise, S.; Briant, T.; Cohadon, P.-F.; Heidmann, A.; Michel, C.; Pinard, L.; Dolique, V.; Flaminio, R.; Taïbi, R.; Chartier, C.; Le Traon, O. Free-space cavity optomechanics in a cryogenic environment. *Appl. Phys. Lett.* **2014**, *104*, 044102.
- [17] Kim, P.H.; Doolin, C.; Hauer, B.D.; MacDonald, A.J.R.; Freeman, M.R.; Barclay, P.E.; Davis, J.P. Nanoscale torsional optomechanics. *Appl. Phys. Lett.* **2013**, *102*, 053102.
- [18] Hossein-Zadeh, M.; Vahala, K.J. Observation of optical spring effect in a microtoroidal optomechanical resonator. *Opt. Lett.* **2007**, *32*, 1611.
- [19] Zheng, Y.; Yu, Q.; Tao, K.; Ouyang, Z. All-optical tunable filters based on optomechanical effects in two-dimensional photonic crystal cavities. *Opt. Lett.* **2013**, *38*, 4362.
- [20] Fang, K.; Matheny, M.H.; Luan, X.; Painter, O. Optical transduction and routing of microwave phonons in cavity-optomechanical circuits. *Nat. Photon.* **2016**, *10*, 489–496.
- [21] Lanzillotti-Kimura, N.D.; Fainstein, A.; Lemaitre, A.; Jusserand, B.; Perrin, B. Coherent control of sub-terahertz confined acoustic nanowaves: Theory and experiments. *Phys. Rev. B* **2011**, *84*, 115453.
- [22] PierantoniMencarelli, L.; Stocchi, D.M. Rigorous simulation of opto-mechanically modulated electromagnetic micro- and nano-cavities. In *Proceedings of the 17th IEEE International Conference on Nanotechnology (IEEE NANO 2017)*, July 25–28, 2017; Pittsburgh, PA, USA.

- [23] Wol, C.; Steel, M.J.; Eggleton, B.J.; Poulton, C.G. Stimulated Brillouin scattering in integrated photonic waveguides: Forces, scattering mechanisms and coupled mode analysis. *Phys. Rev. A* **2015**, *92*, 013836.
- [24] Pendry, J.B.; Schurig, D.; Smith, D.R. Controlling electromagnetic electromagnetic fields. *Science* **2006**, *312*, 1780.
- [25] Schurig, D.; Mock, J.J.; Justice, B.J.; Cummer, S.A.; Pendry, J.B.; Starr, A.F.; Smith, D.R. Metamaterial electromagnetic cloak at microwave frequencies. *Science* **2006**, *314*, 977.
- [26] Zecca, R.; Bowen, P.T.; Smith, D.R.; Larouche, S. Transformation-optics simulation method for stimulated Brillouin scattering. *Phys. Rev. A* **2016**, *94*, 063818.
- [27] Boyd, R.W. *Nonlinear Optics*. Academic Press: Cambridge, MA, 2008.
- [28] Gonzalez, O.; Stuart, A.M. *A Rst Course in Continuum Mechanics*. Cambridge University Press: Cambridge, UK, 2008.
- [29] Qiu, W.; Rakich, P.T.; Shin, H.; Dong, H.; Solja, M.; Wang, Z. Stimulated Brillouin scattering in nanoscale silicon step-index waveguides: A general framework of selection rules and calculating SBS gain. *Opt. Express* **2013**, *21*, 31402.
- [30] Hauer, B.; Doolin, D.C.; Beach, K.S.D.; Davis, J.P. A general procedure for thermomechanical calibration of nano/micro-mechanical resonators. *Ann. Phys.* **2013**, *339*, 181–207.
- [31] Bahl, G.; Tomes, M.; Marquardt, F.; Carmon, T. Observation of spontaneous Brillouin cooling. *Nat. Phys.* **2012**, *8*, 203.
- [32] Navarro-Urrios, D.; Gomis-Bresco, J.; El-Jallal, S.; Oudich, M.; Pitanti, A.; Capuj, N.; Tredicucci, A.; Alzina, F.; Griol, A.; Pennec, Y.; Djafari-Rouhani, B.; Martínez, A.; Sotomayor Torres, C.M. Dynamical back-action at 5.5 GHz in a corrugated optomechanical beam. *AIP Adv.* **2014**, *4*, 124601.
- [33] Gomis-Bresco, J.; Navarro-Urrios, D.; Oudich, M.; El-Jallal, S.; Griol, A.; Puerto, D.; Chavez, E.; Pennec, Y.; Djafari-Rouhani, B.; Alzina, F.; Martínez, A.; Sotomayor Torres, C.M. A one-dimensional optomechanical crystal with a complete phononic band gap. *Nat. Comms.* **2014**, *5*.
- [34] Johnson, S.J.; Ibanescu, M.; Skorobogatiy, M.A.; Weisberg, O.; Joannopoulos, J.D.; Fink, Y. Perturbation theory for Maxwell's equations with shifting material boundaries. *Phys. Rev. E Stat. Nonlin. Soft Matter Phys.* **2002**, *65*, 066611.
- [35] Rakich, P.; Davids, T.P.; Wang, Z. Tailoring optical forces in waveguides through radiation pressure and electrostriction. *Opt. Expr.* **2010**, *18*, 14439–14453.